EPJ manuscript No.
(will be inserted by the editor)

Supplementary Material: Adaptive resolution simulation of an atomistic DNA molecule in MARTINI salt solution

Julija Zavadlav[1,2], Rudolf Podgornik[2,3], Manuel N. Melo[4], Siewert J. Marrink[4], and Matej Praprotnik[1,2,a]

[1] Department of Molecular Modeling, National Institute of Chemistry, Hajdrihova 19, SI-1001 Ljubljana, Slovenia
[2] Department of Physics, Faculty of Mathematics and Physics, University of Ljubljana, Jadranska 19, SI-1000 Ljubljana, Slovenia
[3] Theoretical Physics Department, J. Stefan Institute, Jamova c. 39, SI-1000 Ljubljana, Slovenia
[4] Groningen Biomolecular Sciences and Biotechnology Institute and Zernike Institute for Advanced Materials, University of Groningen, Nijenborgh 7, 9747 AG Groningen, Netherlands

Abstract. The supplementary material of the article.

1 Bundled-SPC/MARTINI NaCl salt solution

In Figure 1 we plot the remaining radial distribution functions (RDFs) — the water oxygen and bundles CoM RDFs. The results are shown for the two monoscale simulations (the fully atomistic and coarse-grained) and the AdResS approach. The RDFs of the AdResS simulation are computed only on atoms located in the respective region of interest, i.e., the atomistic (AdResS AT) or coarse-grained (AdResS CG) domain. All RDFs match the previously reported results [1].

2 DNA Molecule in the multiscale salt solution

The stability of the DNA molecule structure is investigated with the root-mean-square deviation (RMSD) and the root-mean-square fluctuations (RMSF) of the backbone atoms with respect to the average structure. [2] Results are depicted in Figure 2. The DNA molecule remains in a stable configuration during the total simulation time, indicating that the multiscale simulation has no noticeable impact on the averaged DNA structure. Note, that the RMSF vs residue profiles are flat. This is a consequence of periodic boundary conditions for the DNA helix. In simulations of single oligonucleotides the RMSF values of terminal residues are usually found to deviate substantially and affect also the structure of the neighboring residues. [3] This fact further supports our simulation setup mimicking infinitely long DNA molecule.

[a] e-mail: praprot@cmm.ki.si

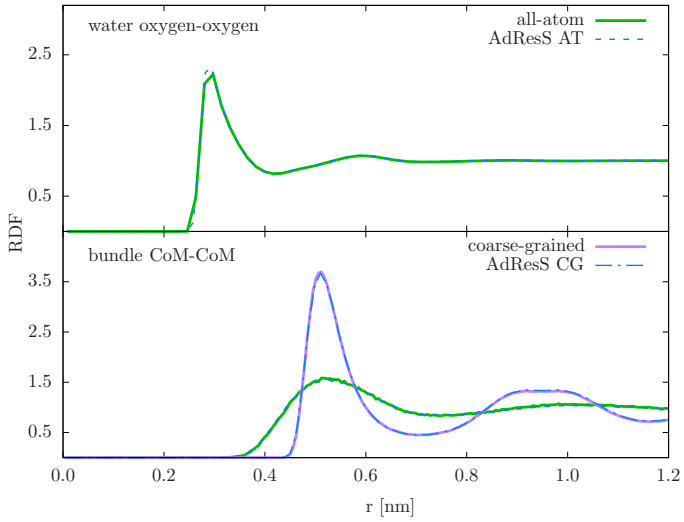

Fig. 1. Radial distribution functions (RDFs) of water oxygen-oxygen (top) and bundles CoM (bottom). The AdResS RDFs are compared with the all-atom and coarse-grained simulation results.

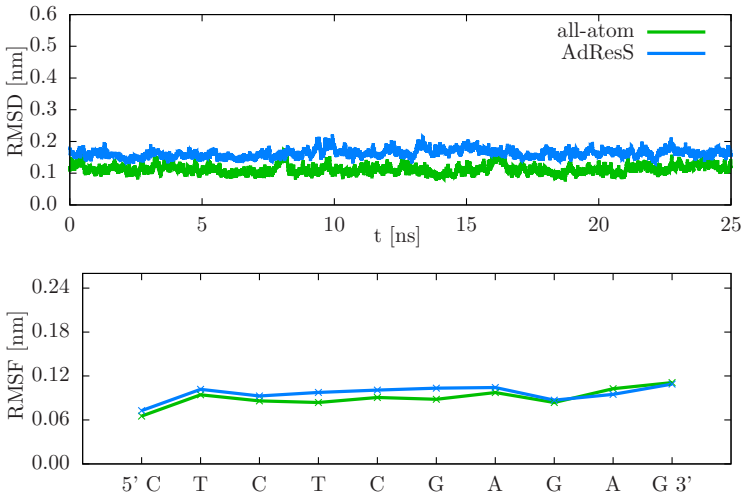

Fig. 2. Root-mean-square deviation (RMSD) and fluctuations (RMSF) of the backbone heavy atoms with respect to the average structure. The A, T, C and G aberrations stand for the adenine, thymine, cytosine, and guanine nucleotides, respectively.

The bundles are not rigid structures, i.e., half-harmonic bonds are used between oxygen atoms. This property is especially important in the vicinity of macromolecules because it allows the water bundles to somewhat deform and adjust to the local structure of the macromolecule. As a means of investigating the internal structure of bundles we use the asphericity (Δ) and radius of gyration (R_g). Asphericity of a

bundle is calculated with [4]

$$\Delta = \frac{3}{2}\frac{\left[\sum_{i=1}^{3}\left(\lambda_i - \frac{\mathrm{tr}\,\mathbf{T}}{3}\right)^2\right]}{\left(\mathrm{tr}\,\mathbf{T}\right)^2} \tag{1}$$

where $\mathbf{T}$ is the inertia tensor of atoms belonging to a certain bundle and λ_i the eigenvalues of $\mathbf{T}$ that define the radius of gyration, i.e., $R_g^2 = \mathrm{tr}\,T = \sum_{i=1}^{3}\lambda_i$. The inertia tensor is computed after centering on the bundle' CoM.

In Figure 3 we plot both properties as a function of distance form DNA's CoM and their probability distribution. The later is shown separately for the bulk AT region,

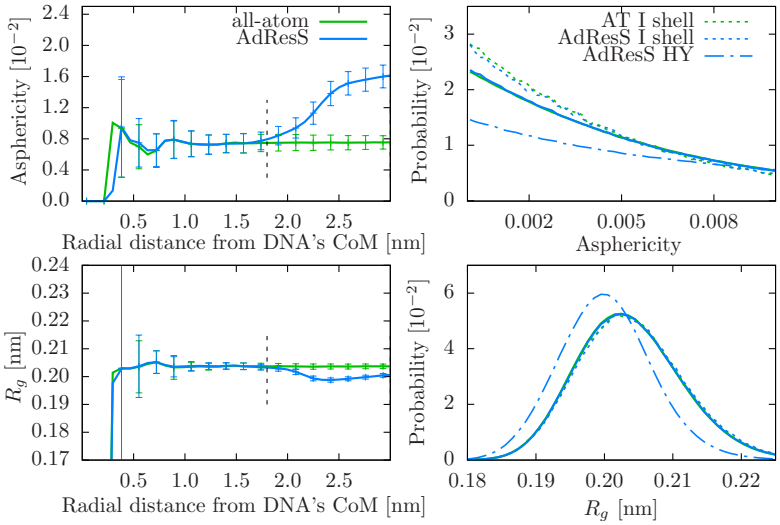

Fig. 3. Left: Asphericity and radius of gyration of bundles with standard deviations as a function of distance form DNA's CoM. The results are plotted for the AT and HY regions with vertical dotted line denoting the boundary. Right: The probability distributions of asphericity and radius of gyration shown separately for the bulk AT region (full), HY region (dash dotted), and bundles in the first hydration shell of the DNA (dotted lines).

HY region, and water bundles in the first hydration shell of the DNA. Small deviations from the mean value can be observed at small separations from DNA's CoM. In this region the standard deviation is quite large due to small number of bundles. But, even so, the AdResS simulation results match the all-atom ones almost to the line thickness. We extract from the asphericity probability distribution that the internal structure of bundles is surprisingly more spherical ($\Delta = 0$ corresponds to a sphere) in the first hydration shell than in the bulk. In the HY region we observe larger discrepancies from the isotropic behavior. However, these discrepancies descend to zero at the AT/HY boundary and thus do not affect the properties of the AT region.

The tetrahedrality order parameter of water surrounding the DNA molecule is shown in Figure 4. The multiscale simulation reproduces the reference all-atom simulation profiles very well. Discrepancies are found only in the HY region where the electrostatic interactions are gradually switched off as the water molecules move from the AT to the CG region. The loss of order is thus to be expected.

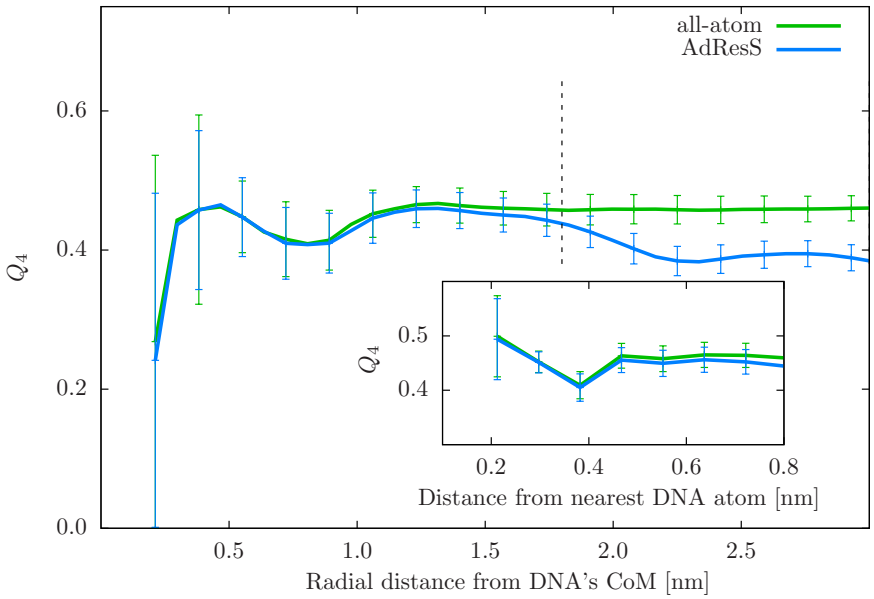

Fig. 4. Tetrahedrality order parameter Q_4 as a function of the radial distance from the DNA's CoM and distance to nearest DNA atom (inset). The results are shown for the AT and HY regions with vertical dotted line denoting the boundary. The error bars represent the standard deviation of the measurements.

Effect of bundling

In this section, we compare the results of the all-atom bundled-SPC and free SPC solvations to elucidate the effect of bundling. In Figure 5 we plot the water-water, water-ion and ion-ion RDFs. The water-ions RDFs match within the line thickness, while some differences are found for the water-water and ion-ion RDFs.

In Figure 6 we show the RMSD and RMSF values of the DNA's backbone heavy atoms. The RMSF values for the DNA molecule in the free SPC solvation are larger, indicating a more flexible backbone chain. A reasonable explanation could be the viscosity difference of water models. The reported viscosities are 0.85 and 0.5 mPa s [5] for the bundled-SPC and free SPC water models, respectively.

The average number and lifetime of the observed hydrogen bonds between the DNA and water are shown in Figure 7. Both solvations give very similar results, which confirms that the bundling most strongly affects the self-interactions of the water molecules while the interactions with other molecules are mostly unchanged.

Figure 8 shows the distributions of the tetrahedrality order parameter. We compute separately the distributions for the water molecules located in the first solvation shell around the DNA molecule and the bulk water (beyond the first shell). On the basis of proximity analysis water molecules the first shell are assigned to either minor or major groove or the backbone. If only water molecules are considered in the calculation of Q_4, the distribution profiles of the first hydration shell and the bulk differ substantially. However, with the included DNA atoms all distributions match. Note that the distributions of the free SPC and bundled-SPC solvations are not the same.

It is known that the diffusion of the bundled-SPC water ($\approx 1.2 \times 10^9$ [5]) is slower than that of the free SPC water ($\approx 4.2 \times 10^9$ m^2 s^{-1} at 300 K [5]) due to the larger hydrodynamic radius of the bundles compared to the single SPC molecules.

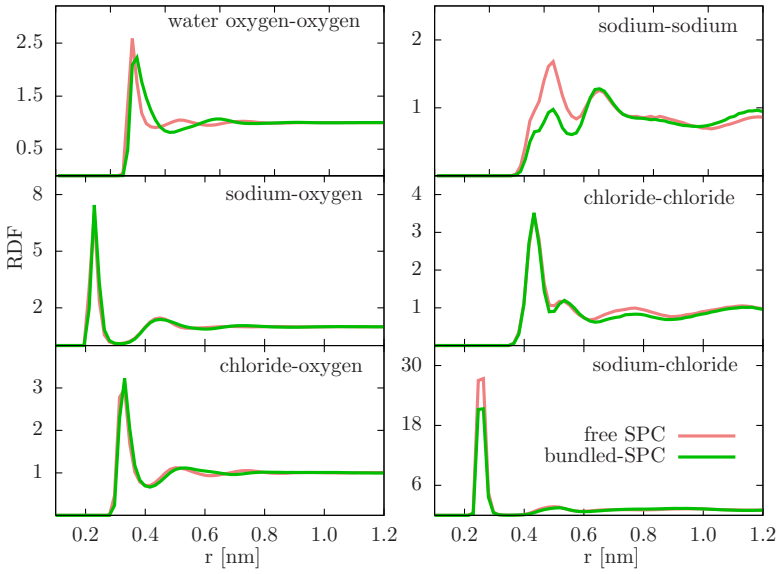

Fig. 5. Radial distribution functions (RDFs) of water oxygen-oxygen, sodium-oxygen, chloride-oxygen, sodium-sodium, chloride-chloride, and sodium-chloride. We compare the results of all-atom simulations with either free SPC or bundled-SPC water model.

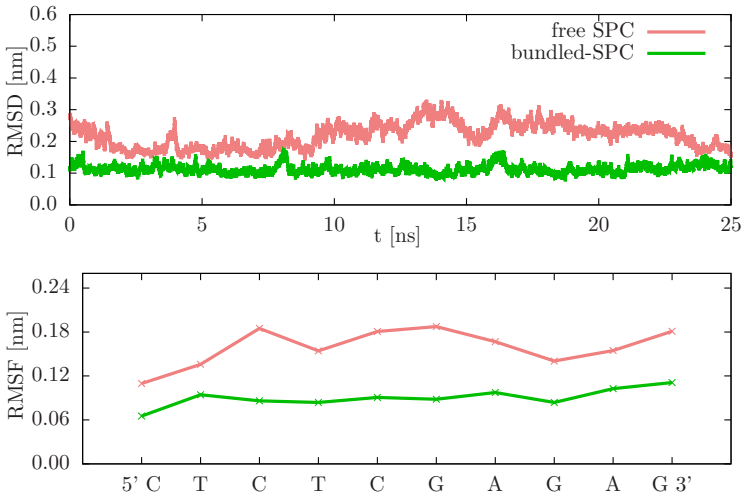

Fig. 6. Root-mean-square deviation (RMSD) and fluctuations (RMSF) of the backbone heavy atoms with respect to the average structure. The A, T, C and G abbreviations stand standardly for the adenine, thymine, cytosine, and guanine nucleotides, respectively.

To determine whether the "bundling" also affects the rate of the water molecule's reorientation we compute the dipole autocorrelation function d_{ACF}. The results are plotted in Figure 9.

We examine independently the water molecules that are at time $t = 0$ located in the first hydration shell around the DNA molecule — these are assigned to the minor, major groove or backbone region based on the proximity analysis — or in the bulk.

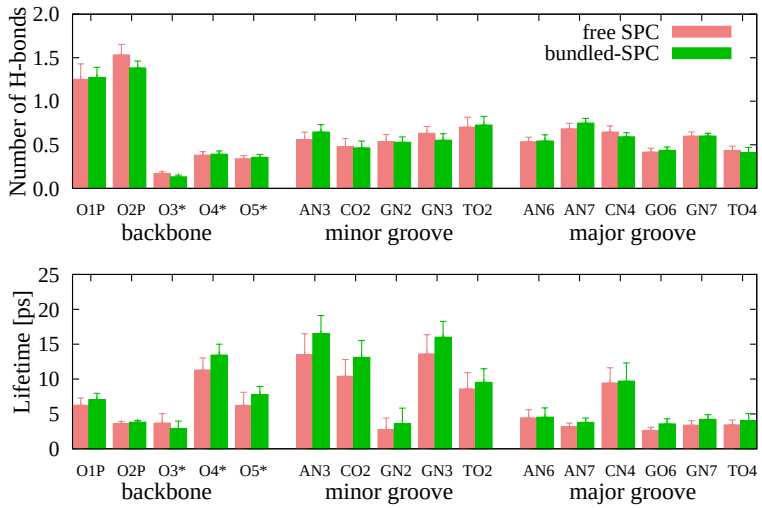

Fig. 7. Average number (top) and lifetime (bottom) of hydrogen bonds occurring between the DNA atoms and water. The results are shown separately for the selected electronegative nitrogen and oxygen atoms of the DNA.

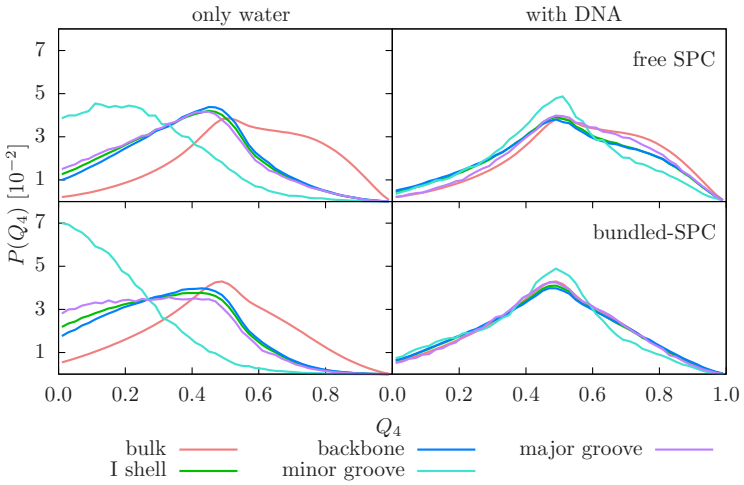

Fig. 8. Distribution of the tetrahedrality order parameter $P(Q_4)$ for the bulk water and first solvation shell around the DNA molecule. Additionally, the water molecules in the first solvation shell are further distinguished on the basis of their proximity to either minor or major groove or the backbone.

We find that the characteristic times of water reorientation in all regions are alike for all performed simulations indicating that the half-harmonic bonds do not change the rotational diffusion. In accordance with previous simulations [7] we observe the slowest decay of d_{ACF} for water molecules in the minor groove. Here, the slowing down of rotational motion could be pronounced due to low density of water [8].

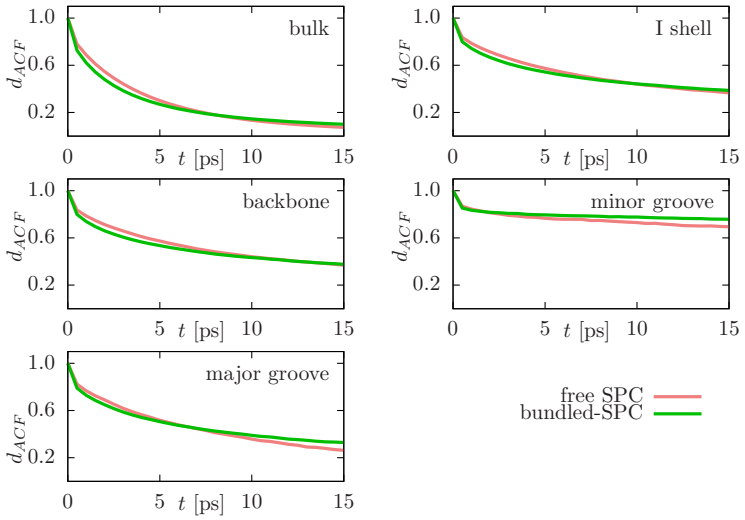

Fig. 9. Dipole autocorrelation function d_{ACF} as a function of time. We average over water molecules that are initially in the first hydration shell of DNA and over water molecules that are further away but still in the AT region [6]. On the basis of proximity analysis water molecules are further assigned to either minor or major groove or the backbone.

References

1. J. Zavadlav et al., J. Chem. Theory Comput. **10**, 2591 (2014).
2. M. Nina and T. Simonson, J. Phys. Chem. B **106**, 3696 (2002).
3. R. Lavery et al., Nucleic Acids Res. **38**, 299 (2010).
4. R. I. Dima and D. Thirumalai, J. Phys. Chem. B **108**, 6564 (2004).
5. M. Fuhrmans, B. P. Sanders, S. J. Marrink, and A. H. de Vries, Theor. Chem. Acc. **125**, 335 (2010).
6. L. Delle Site, Phys. Rev. E **93**, 022130 (2016).
7. J. Zavadlav, R. Podgornik, and M. Praprotnik, J. Chem. Theory Comput. **11**, 5035 (2015).
8. J. T. Titantaha and M. Karttunen, Soft Matter **11**, 7977 (2015).